Radioactivity of neutron-rich oxygen, fluorine, and neon isotopes

A. T. Reed,[1] O. Tarasov,[2] R. D. Page,[1] D. Guillemaud-Mueller,[3] Yu. E. Penionzhkevich,[2] R. G. Allatt,[1] J. C. Angélique,[4] R. Anne,[5] C. Borcea,[6] V. Burjan,[7] W. N. Catford,[8] Z. Dlouhý,[7] C. Donzaud,[3] S. Grévy,[3,*] M. Lewitowicz,[5] S. M. Lukyanov,[2] F. M. Marqués,[4] G. Martinez,[5,†] A. C. Mueller,[3] P. J. Nolan,[1] J. Novák,[7] N. A. Orr,[4] F. Pougheon,[3] P. H. Regan,[8] M. G. Saint-Laurent,[5] T. Siiskonen,[9] E. Sokol,[2] O. Sorlin,[3] J. Suhonen,[9] W. Trinder,[5] and S. M. Vincent[8,‡]

[1]*Oliver Lodge Laboratory, University of Liverpool, Liverpool L63 7ZE, United Kingdom*

[2]*Flerov Laboratory of Nuclear Reactions, Joint Institute for Nuclear Research, 141980 Dubna, Moscow Region, Russia*

[3]*Institut de Physique Nucléaire, CNRS-IN2P3, F-91406 Orsay Cedex, France*

[4]*Laboratoire de Physique Corpusculaire, CNRS-IN2P3, ISMRA et Université de Caen, F-14050 Caen Cedex, France*

[5]*Grand Accélérateur National d'Ions Lourds, BP 5027, F-14076 Caen Cedex 5, France*

[6]*Institute of Atomic Physics, Bucharest-Magurele, P.O. Box MG6, Romania*

[7]*Nuclear Physics Institute, 250 68 Rez, Czech Republic*

[8]*Department of Physics, University of Surrey, Guildford GU2 5XH, United Kingdom*

[9]*Department of Physics, University of Jyväskylä, FIN-40351 Jyväskylä, Finland*

(Received 1 February 1999; published 20 July 1999)

The γ radiation and neutrons emitted following the β decays of ^{24}O, $^{25-27}$F, and $^{28-30}$Ne have been measured. The nuclides were produced in the quasifragmentation of a 2.8 GeV ^{36}S beam, separated in-flight and identified through time-of-flight and energy-loss measurements. The ions were stopped in a silicon detector telescope, which was used to detect the β particles emitted in their subsequent radioactive decay. The coincident γ rays were measured using four large volume germanium detectors mounted close to the implantation point and the neutrons were detected using 42 ^{3}He proportional counters. The measured γ-ray energy spectra are compared with shell model calculations and, where available, the level energies deduced from multinucleon transfer reactions. [S0556-2813(99)04108-4]

PACS number(s): 21.60.Cs, 23.20.Lv, 23.40.−s, 27.30.+t

I. INTRODUCTION

Nuclei possessing neutron/proton ratios radically different from those of stable isotopes exhibit unexpected phenomena which have revolutionized our understanding of nuclear physics. Properties such as neutron halos and the modification of shell closures are predicted for a wide range of extremely neutron-rich nuclei, but it is only for the lightest elements that nuclei at the neutron drip line can presently be accessed experimentally. Although the neutron drip line has probably been delimited for elements below neon [1,2] and the atomic masses of many of these nuclei measured [3,4], comparatively little is known about their decay characteristics or spectroscopy [5]. Such measurements can probe important details of the underlying microscopic structures which give rise to the novel phenomena.

The energy spectra of excited levels for certain nuclei reasonably close to stability have been measured using transfer reactions [6–10], but rapidly diminishing cross sections limit the range of nuclei which are amenable to study using this approach. A complementary tool is β-delayed γ-ray spectroscopy, which can probe a different subset of excited states and, provided the decay schemes can be interpreted, can measure level energies with a greater precision. In principle β-decay measurements can be applied to nuclei right up to the neutron drip line, as long as the nuclei of interest can be cleanly and efficiently separated and their radioactivity measured with high sensitivity.

In the present work, β-delayed γ-ray and neutron emission has been studied for the first time in a range of neutron rich nuclei extending out to the $A/Z=3$ nuclides $^{24}_{8}$O, $^{27}_{9}$F, and $^{30}_{10}$Ne.

II. EXPERIMENTAL TECHNIQUE

The neutron rich nuclei of interest were produced by the quasifragmentation of a 0.5 $e\mu$A 2.8 GeV beam of the rare isotope $^{36}S^{16+}$ on tantalum targets of thicknesses 288 μm, 377 μm, 539 μm, and 854 μm, mounted on $\sim$100 μm thick carbon backings. The two thinner targets were mounted on a rotating wheel. Five different settings of the LISE3 spectrometer [11] were used to optimize the collection of different nuclei in turn, by adjusting the magnetic rigidity of the first section of LISE3 to transmit ions that would have the correct magnetic rigidity after passing through the 553 μm thick achromatic beryllium degrader. The achromatic degrader and all subsequent elements of the spectrometer were left unchanged throughout the rest of the experiment, thereby minimizing the time taken for each adjustment but still producing satisfactory collection rates for the nuclei of interest.

The selected nuclei were implanted into a stack of six silicon detectors located at the focal plane of LISE3. The first

*Present address: Laboratoire de Physique Corpusculaire, CNRS-IN2P3, ISMRA et Université de Caen, F-14050 Caen Cedex, France.

†Present address: SUBATECH, IN2P3-CNRS et Ecole des Mines de Nantes, F-44070 Nantes Cedex 03, France.

‡Present address: Department of Physics, University of Notre Dame, Notre Dame, Indiana 46556.

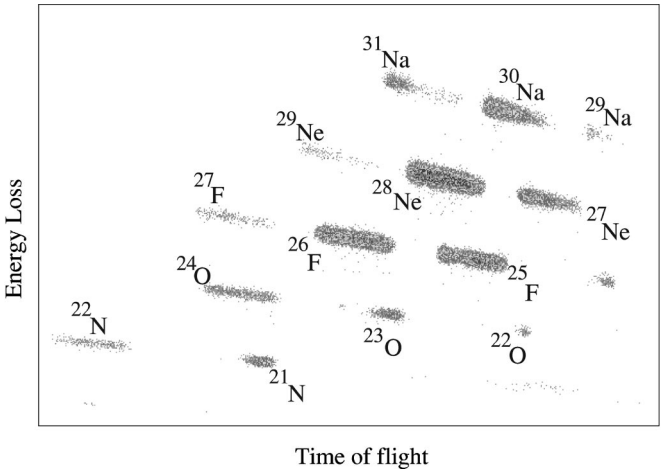

FIG. 1. Two-dimensional ion identification spectrum showing time of flight plotted against energy loss for ions observed with the LISE3 spectrometer optimized for the transmission of ^{26}F. Each cluster of counts corresponds uniquely to a specific nuclide and the most strongly transmitted nuclides are labeled.

detector was 500 μm thick and provided energy-loss and timing signals, which were used to identify the ions on an event-by-event basis. The ions subsequently passed through silicon detectors of thickness 500 μm, 300 μm, and 500 μm, which provided redundant identification. The ion identification spectrum obtained with LISE3 optimized for the transmission of ^{26}F is shown in Fig. 1.

The final two detectors were 5 mm thick lithium drifted silicon detectors. The ions were stopped in the fifth element of the silicon detector telescope, while the sixth detector was used to veto light ions which were transmitted to the focal plane of LISE3 and passed through the fifth detector. The last three detectors were also used to detect β particles emitted in the radioactive decay of the implanted nuclei using a second set of shaping amplifiers with a high gain. The efficiency for β-particle detection was determined to be 63 $\pm$4% from the known decays of ^{30,31}Na, which were implanted during the experiment.

The silicon detector telescope was surrounded on three sides by 42 cylindrical ^{3}He proportional counters [12], each encased in a polyethylene moderator, which were used to measure β-delayed neutron emission probabilities. The total efficiency of these detectors was determined to be 14% from the decays of the known β-delayed neutron emitters ^{30,31}Na which were produced during the experiment.

The energies of γ rays emitted following β decay were measured using four tapered germanium detectors, each of 70% relative efficiency [13], mounted in close proximity to the implantation point around 0° to the secondary beam direction. The germanium detectors were not housed in Compton suppression shields, in order to achieve a close-packed geometry, but were wrapped in lead foil to reduce cross scattering of γ rays between the detectors. The thickness of the wall of the aluminum vacuum vessel containing the silicon detectors was only 0.5 mm, thus minimizing the attenuation of the γ rays. The combined efficiency of the four germanium detectors was measured to be 2.1$\pm$0.1% at 1.33 MeV. The low energy thresholds of these detectors were set to $\sim$100 keV.

The typical ion implantation rates of <5 s^{-1} and the short half-lives of the nuclides of interest meant that the experiment was run in a continuous mode of implantation. A clock running at 10 kHz was used to time stamp all ion implantation and β-decay events in order to allow the measurement of half-lives. In cases where strong β-delayed γ-ray lines were identified, decay curves were generated from the time differences between the arrival of the ions and the detection of their β-delayed γ rays. By measuring half-lives using this technique, both the ion and the correlated β-decay event can be cleanly and unambiguously selected, thereby greatly reducing the problems of random correlations which can be encountered when only β particles are detected. These random correlations of ions with unrelated β decays are particularly evident for longer-lived nuclides and in several cases a fraction of the total β-delayed γ-ray energy spectrum for the relevant spectrometer setting has been subtracted to demonstrate which γ rays are really associated with the decay. This fraction was determined from the relative yields of the random γ rays in the spectra, but in all cases the absolute γ ray intensities were measured from the unsubtracted spectra.

III. RESULTS AND DISCUSSION

In the following sections the first β-delayed γ-ray measurements for ^{24}O, $^{25-27}$F, and $^{28-30}$Ne are presented. Possible level schemes deduced from the γ-ray spectra are compared with the results of transfer reaction studies and shell model calculations. The half-lives and neutron emission probabilities measured for these nuclides are summarized in Table I. In addition, a first half-life measurement was also obtained for ^{19}B in the present experiment and this value is included in Table I.

A. The decay of ^{24}O

No excited states were previously known in ^{24}F, the β-decay daughter of the heaviest bound oxygen isotope ^{24}O [1,2]. In the β-delayed γ-ray energy spectra for ^{24}O ions shown in Fig. 2, the peak at 1982 keV is assigned as the known $2^+ \rightarrow 0^+$ transition energy in ^{24}Ne populated in the β decay of ^{24}F [18]. There is no correspondence between the remaining γ-ray energies identified in these spectra and the energies of known levels in ^{23}F [10], suggesting that the γ rays are emitted from levels in ^{24}F, rather than ^{23}F following neutron emission. This conclusion is supported by the value of 12$\pm$8% measured for the β-delayed neutron emission probability of ^{24}O using the ^{3}He proportional counters. Another independent estimate of the neutron emission probability was determined from the yield of the 1982 keV γ ray, which indicates that 76$\pm$8% of the ^{24}O β decays eventually feed the ^{24}F ground state, rather than leading to neutron emission. The previous measurement of the β-delayed neutron emission probability of ^{24}O yielded a value of 58 $\pm$12% [14], which is much higher than both of the values deduced in the present work.

TABLE I. Summary of half-life and β-delayed neutron emission probability measurements from the present work compared with previous measurements where available. The half-lives were determined in the present work by gating on β-delayed γ rays as described in the text, except for the cases of ^{19}B and ^{27,29}F, for which the time differences between the arrival of the ions and the next β decay were used.

Nuclide	Number of ions	Half-life (ms)		Neutron emission probability (%)	
		This work	Literature	This work	Literature
^{19}B	340	4.5 ± 1.5			
^{24}O	9000	65 ± 5	$61\ ^{+32}_{-19}$ [14]	18 ± 6	58 ± 12 [14]
^{25}F	40000	50 ± 6	59 ± 40 [15]	14 ± 5	15 ± 10 [15]
^{26}F	50000	10.2 ± 1.4		11 ± 4	
^{27}F	10000	6.5 ± 1.1	5.3 ± 0.9 [1]	$90\ ^{+10}_{-30}$	
			4.9 ± 0.2 [16]		
^{29}F	650	2.9 ± 0.8	2.4 ± 0.8 [1]		
			2.6 ± 0.4 [16]		
^{28}Ne	105000	18 ± 3	16 ± 9 [15]		
			17 ± 4 [17]		
			21 ± 5 [1]		
^{29}Ne	8600	19 ± 9	15 ± 3 [1]	27 ± 9	
			15.6 ± 0.5 [16]		
^{30}Ne	3000	7 ± 2	7 ± 2 [1]		
			5.8 ± 0.2 [16]		

The half-lives determined for each of the γ-ray lines assigned to the decay of ^{24}O to ^{24}F are mutually consistent. Fitting the combined data yields a half-life of 65 ± 5 ms, which compares with the previously reported value of 61^{+32}_{-19} ms [14].

The energies and intensities of the three γ rays attributed to transitions in ^{24}F populated in the β decay of ^{24}O are listed in Table II. The sum of the energies of the two lower energy lines equals that of the highest energy line within the uncertainties, suggesting that these transitions represent two separate decay paths between a common initial and final state. It is not possible to determine the relative ordering of the 522 keV and 1310 keV γ rays on the basis of the intensities, which suggests that there is little or no feeding of the intermediate level connecting these transitions.

The energy spectrum of excited states in ^{24}F has been calculated using the Michigan State University version of the shell model code OXBASH [19] using three different interactions proposed for *sd* shell nuclei [20–22]. The calculated level structures are shown in Fig. 3, from which it is evident that all three interactions predict the same sequence of lowest-lying levels although the precise energies of the levels differ. A possible partial level scheme consistent with the γ rays identified in Fig. 2 is compared with these shell model calculations in Fig. 3. The tentative ordering of the 1310 keV and 522 keV transitions provides better agreement with the shell model calculations, which also predict that the lowest 1^+ level is strongly populated in the β decay.

Within this level scheme, the absolute feeding intensity of the 1832 keV level is $40.3\pm4.0\%$. Taking the β-decay Q value between the ground states to be $11\,430\pm315$ keV [23], this corresponds to a logft value of $4.30\ \pm0.13$, which is consistent with an allowed transition. Combining the average

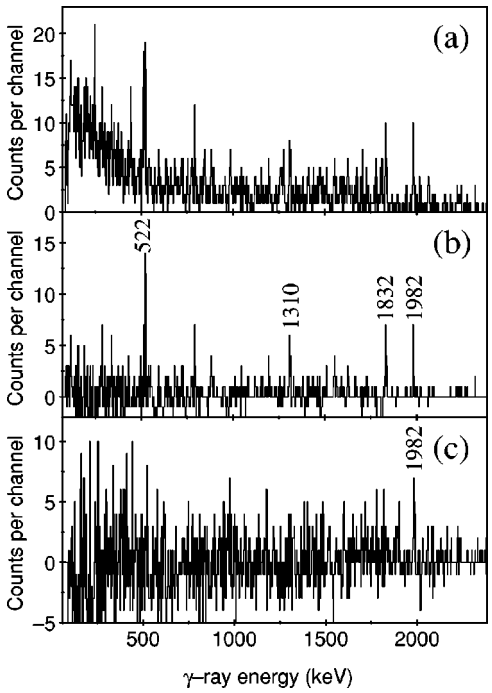

FIG. 2. Energy spectra of (a) all β-delayed γ rays occurring within 200 ms of the implantation of a ^{24}O ion; (b) the same spectrum following the subtraction of a fraction of the total β-delayed γ-ray spectrum observed at this setting of the LISE3 spectrometer; and (c) the background subtracted energy spectrum of β-delayed γ rays occurring between 200 ms and 1 s after the arrival of a ^{24}O ion. γ-ray peaks associated with the β decay of ^{24}O and its daughter ^{24}F are labeled according to their energy in keV. The energy spectrum shown in (c) clearly shows a vestige of the 1982 keV line from the decay of ^{24}F ($t_{1/2}=340\pm80$ ms [18]), whereas the other three lines present in (b) have decayed away.

TABLE II. Energies and intensities of γ rays observed in the β decay of ^{24}O to ^{24}F, corrected for the β-delayed γ-ray detection efficiency.

E_γ (keV)	I_γ (relative)	I_γ (per 100 decays)
521.5±0.3	50.3±8.7	14.3±2.0
1309.5±0.5	43.2±10.6	12.0±2.6
1831.6±0.5	100.0±10.7	28.3±3.0

of the β-delayed neutron emission probabilities measured in the present work and the observed β-decay strength feeding the proposed level at 1832 keV, approximately 40% of the total decay strength remains unaccounted for. However, the shell model level calculations predict another bound 1^+ level at around 3 MeV. If this level were mainly to decay directly to the ground state, the efficiency for detecting the emitted γ rays in coincidence with a β particle would be rather low ($\approx 0.2-0.4\%$) and hence may not have been observed.

B. The decay of ^{25}F

Although the β-delayed neutron emission and half-life of ^{25}F have been measured [15], the γ rays emitted following the β decay of this nuclide have not been previously studied. Several γ-ray lines are evident in the spectrum of Fig. 4(c), in addition to the 1982 keV $2^+ \rightarrow 0^+$ transition in ^{24}Ne [18] populated in this case following the emission of a neutron. None of these γ-ray energies correspond to transitions in the grand-daughter nuclide ^{25}Na, [24] so they are attributed to γ rays emitted from levels in ^{25}Ne which are populated in the β decay of ^{25}F. The absolute intensities of the γ rays are presented in Table III.

The half-lives extracted for the three most intense γ-ray lines are mutually consistent and combining the lifetime data yields a value of 50±6 ms for the half-life of ^{25}F, which is consistent with the previous value of 59±40 ms [15]. The

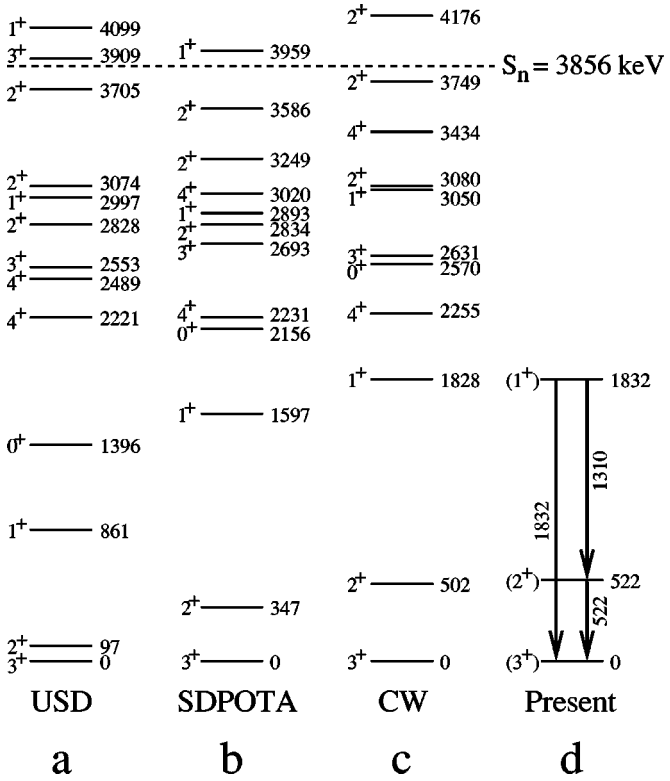

FIG. 3. Energy levels of ^{24}F up to ~4 MeV calculated using the shell model code OXBASH [19] with (a) the USD interaction [21]; (b) the SDPOTA interaction [22]; and (c) the interaction of Chung and Wildenthal [20], compared with the tentative partial level scheme deduced in the present work. The energies of the levels and γ rays are given in keV and the tentative spin and parity assignments for the deduced levels are in parentheses. The one neutron separation energy [23] is indicated by the dashed line.

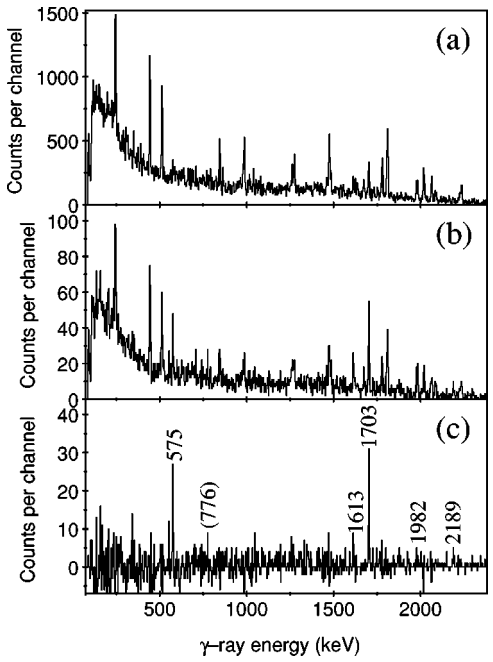

FIG. 4. Energy spectra of (a) all β-delayed γ rays observed at the LISE3 spectrometer setting used to study the decay properties of ^{25,26}F; (b) all β-delayed γ rays occurring within 200 ms of the arrival of a ^{25}F ion at the focal plane of LISE3; and (c) the same spectrum after the subtraction of a normalized fraction of the total spectrum (a). γ rays associated with the β decay of ^{25}F are labeled with their energy in keV. The 1982 keV γ-ray line is significantly broader than others of similar energy (9±1 keV FWHM compared with 4±1 keV FWHM), which is compatible with the Doppler broadening expected following the emission of a ~1.4 MeV neutron.

TABLE III. Energies and intensities of γ rays observed in the β decay of ^{25}F, corrected for the β-delayed γ-ray detection efficiency.

E_γ (keV)	I_γ (relative)	I_γ (per 100 decays)
574.7±0.5	24.3±2.8	9.5±0.9
1613.4±1.2	29.8±5.0	11.6±1.8
1702.7±0.7	100±6.7	39.1±2.6
2188.6±1.3	18.5±4.3	7.2±1.6

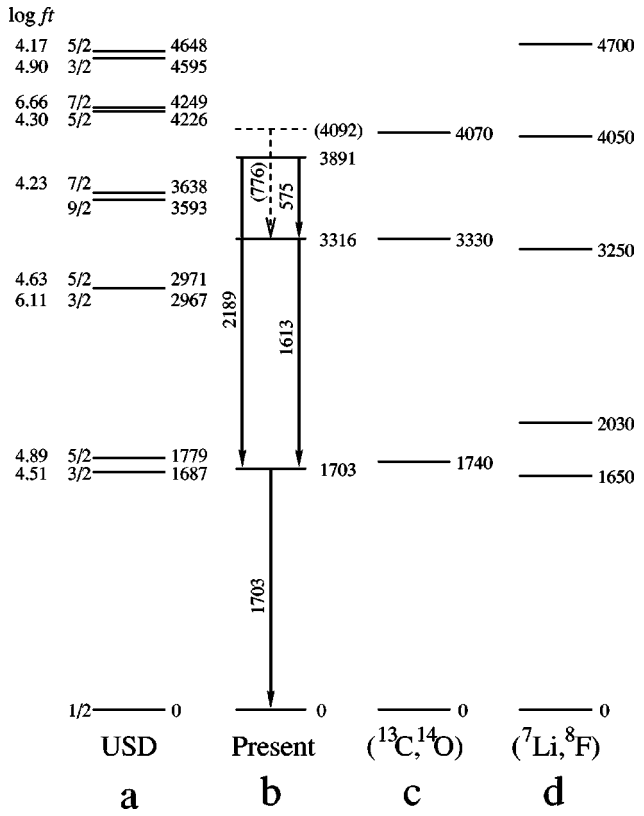

FIG. 5. Comparison of (a) energy levels of ^{25}Ne predicted using the shell model with the USD interaction [21], including calculated log*ft* values; (b) the partial level scheme deduced in the present work; (c) the energy levels identified by Woods *et al.* [9]; and (d) the energy levels measured by Wilcox *et al.* [6]. The dashed lines and values in parentheses indicate tentative levels and transitions. The excitation energies of the levels and γ-ray transition energies are given to the nearest keV. The uncertainties on the level energies shown in (c) are all ± 30 keV, while those of the excited levels shown in (d) are, in order of increasing energy, ± 50 keV, ± 50 keV, ± 80 keV, ± 80 keV, and ± 100 keV. The level observed at 6.28 ± 0.05 MeV in Ref. [9] is not shown. See text for details of the widths of the levels measured in [9].

β-delayed neutron emission probability of ^{25}F was determined as $14 \pm 5\%$ from the signals observed in the neutron detectors, which is also consistent with the previously measured value of $15 \pm 10\%$ [15]. This compares with the absolute intensity of $11 \pm 3\%$ measured for the 1982 keV transition, which can be regarded as a lower limit for the β-delayed neutron emission probability of ^{25}F.

The energy level spectrum of ^{25}Ne has previously been studied by Wilcox *et al.* using the reaction ^{26}Mg(^{7}Li,^{8}B)^{25}Ne [6] and later by Woods *et al.* using the reaction ^{26}Mg(^{13}C,^{14}O)^{25}Ne [9] (see Fig. 5). The latter experiment found no evidence for peaks at 2.03 MeV or 4.7 MeV seen in the earlier study, and the two lowest energy peaks at 1.74 MeV and 3.33 MeV each possibly comprised two unresolved components, separated by ~ 110 keV and ~ 200 keV, respectively. The differences between the two studies are discussed in [9].

Shell model calculations for ^{25}Ne using the USD interaction [21] predict two levels close to an excitation energy of 1.7 MeV (see Fig. 5), both of which could be populated directly by allowed β decays from the $J^{\pi} = 5/2^{+}$ ground state of ^{25}F. On the basis of reaction mechanism considerations and calculated spectroscopic factors, Woods *et al.* argued that the peak they observed at 1.74 MeV was probably mostly due to the $3/2^{+}$ level predicted at 1687 keV. The shell model calculations predict that this level should be more strongly populated in the β decay than the predicted 1779 keV $5/2^{+}$ level, suggesting that the 1703 keV γ ray, which is the most intense line observed in the present work, could represent the decay of this $3/2^{+}$ level to the ground state. The energy of this level would be consistent with those observed in both transfer reaction studies.

TABLE IV. Energies and feeding intensities of energy levels in ^{25}Ne tentatively deduced from the β decay of ^{25}F, corrected for the β-delayed γ-ray detection efficiency. The Q_{β} value between ground states has been taken as $13\,325 \pm 89$ keV [23].

E_{level} (keV)	Feeding intensity (%)	log*ft*
3890.8 ± 1.5	16.9 ± 1.8	4.54 ± 0.11
3316.1 ± 1.4	2.2 ± 2.0	5.55 ± 1.15
1702.7 ± 0.7	20.0 ± 3.5	4.92 ± 0.13

The energies of the 575 keV, 1613 keV, and 2189 keV transitions suggests that these γ rays form different decay paths between common states. Although the 1613 keV γ ray could represent the decay of the second level predicted near 1.7 MeV, no shell model states are expected near 2.2 MeV. Alternatively, the 1613 keV transition could represent the decay of a level at 3316 keV, the energy of which would be consistent with those observed in the transfer measurements (see Fig. 5). One difference is that Woods *et al.* argue that the broad peak they observed probably arises mainly from the $3/2^{+}$ level predicted at 2967 keV, whereas the calculated log*ft* values suggest that the $5/2^{+}$ level at 2971 keV would be much more strongly populated in the β decay of ^{25}F.

The 575 keV and 2189 keV γ rays could deexcite a level at 3891 keV. Although this energy is inconsistent with that of the 4.07 ± 0.03 MeV level [9], the shell model predicts levels at 3638 keV and 4226 keV that should be strongly populated by β decay. The level energies and feeding intensities are summarized in Table IV, together with the log*ft* values deduced assuming the level scheme shown in Fig. 5. Each log*ft* value is consistent with an allowed β decay and all of the proposed levels lie below the neutron emission threshold of 4183 ± 46 keV [23].

A fifth γ-ray line that could only be tentatively assigned to a transition in ^{25}Ne was identified at an energy of 776.3 ± 0.3 keV, with an intensity of 1.7 ± 0.6 γ rays per 100 ^{25}F β decays. If this γ ray were to feed the 3316 keV level it would imply a state at 4092 keV, consistent with both transfer measurements. The apparent absence of direct β-decay feeding of the 3316 keV level could be explained by the low γ-ray detection efficiency ($\approx 0.3\%$) if this level decays directly to the ground state, or a decay branch via the expected $5/2^{+}$ level near 1.7 MeV.

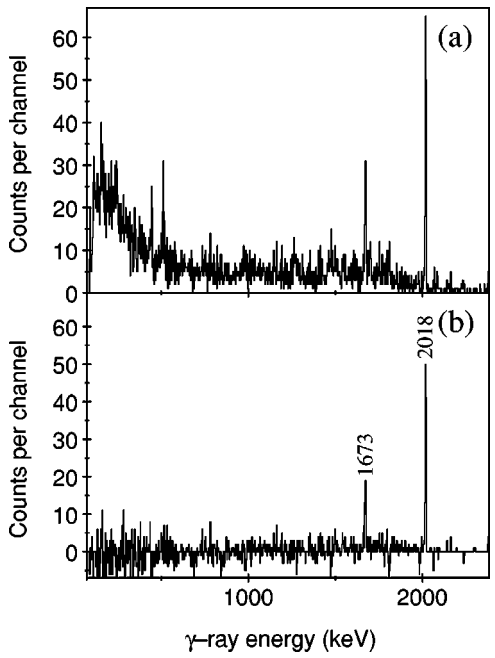

FIG. 6. Energy spectra of (a) all β-delayed γ rays occurring within 50 ms of the arrival of a ^{26}F ion at the focal plane of LISE3 and (b) the same spectrum after the subtraction of a normalized fraction of the total β-delayed γ-ray spectrum for this LISE3 setting shown in Fig. 4(a). γ-ray lines associated with the decay of ^{26}F are labeled according to their energy in keV in the lower spectrum.

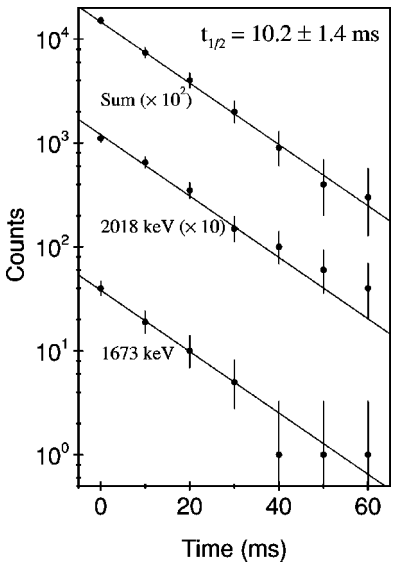

FIG. 7. Decay curves for the two γ-ray transitions assigned to the β decay of ^{26}F to levels in ^{26}Ne and the sum of these data. The half-life of 10.2 ± 1.4 ms was determined from a maximum likelihood fit to the combined data from the two transitions.

The observed γ rays in the tentative level scheme of Fig. 5 and the measured β-delayed neutron emission probablity together account for only $53\pm8\%$ of the total decay strength. In addition to the unobserved transitions discussed above, the detection efficiency for the possible level at 4092 keV decaying directly to the ground state would be only $\approx0.2\%$, while feeding of a second level near 3.3 MeV could be expected from the transfer measurements [9] and shell model calculations. Clearly a further experiment with a greater efficiency for high-energy γ rays is required to establish whether these are sufficient to account for the remaining decay intensity.

C. The decay of ^{26}F

The mass of ^{26}F has been measured [3,4], but its β-decay properties have not previously been investigated. The β-delayed γ-ray energy spectra of Fig. 6 contain two prominent γ-ray lines at energies that do not correspond to those previously measured for the β decays of the daughter nuclides ^{25,26}Ne [18,24], or those reported above for the decay of ^{25}F. These γ-ray lines are therefore attributed to transitions from excited states in ^{26}Ne populated in the β decay of ^{26}F.

The decay curves obtained for these γ rays are shown in Fig. 7. The half-lives obtained from these data are mutually consistent and combining the data results in a first half-life measurement of 10.2 ± 1.4 ms for ^{26}F.

The absolute intensities of the 1673 keV and 2018 keV γ-ray transitions are presented in Table V. The relative intensities of the two lines and the absence of any other strong γ-ray lines clearly indicate that both levels are populated directly in the β decay. The experimental level scheme is compared with spherical shell model calculations in Fig. 8. The shell model calculations predict that the ground state of ^{26}F has $J^\pi=1^+$, which would suggest that the 3691 keV level has $J^\pi=0^+$ or 2^+, assuming allowed β-decay transitions predominate.

The daughter nuclide ^{26}Ne has previously been studied using the double charge exchange reaction ^{26}Mg$(\pi^-,\pi^+)^{26}$Ne [7]. In addition to observing the ground state, evidence was obtained for a peak comprising eight events at an excitation energy of ~3.75 MeV. From the kinematic constraints of the experimental technique, it was concluded that this was probably a 0^+ level. Since we would expect to observe this level in our measurement, assuming a $J^\pi=1^+$ ground state for ^{26}F, but no γ rays attributable to other levels in this energy region are evident in our spectrum, we tentatively assign the 3691 keV level as the previously observed 0^+ level. This interpretation is reinforced by a comparison with the level scheme of ^{28}Mg [25], deduced from the β decay of the $J^\pi=1^+$ ground state of ^{28}Na [26], in which the two most strongly populated excited levels are the first and second excited states with $J^\pi=2^+$ and 0^+, respectively. If the relative feeding strength of the second excited 2^+ level in the decay of ^{26}F were similar to that in the

TABLE V. Energies and intensities of γ rays observed in the β decay of ^{26}F, corrected for the β-delayed γ-ray detection efficiency.

E_γ (keV)	I_γ (relative)	I_γ (per 100 decays)
1673.0 ± 0.3	27.7 ± 4.1	18.7 ± 2.2
2018.2 ± 0.1	100.0 ± 9.2	67.3 ± 5.8

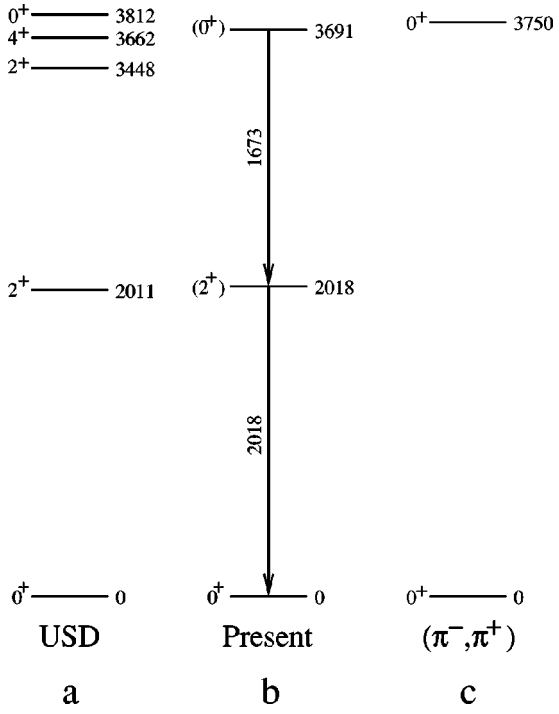

FIG. 8. Comparison of (a) energy levels of ^{26}Ne predicted using the shell model with the USD interaction [21]; (b) the partial level scheme deduced in the present work; and (c) the energy levels identified by Nann *et al.* [7]. The excitation energies of the levels and γ-ray transition energies are given to the nearest keV. The spin and parity values in parentheses indicate tentative assignments.

decay of its isotone ^{28}Na, the γ-ray intensity from this level to the ground state of ^{26}Ne would be below the sensitivity limits of the present experiment.

The β-delayed neutron emission probability of ^{26}F was measured for the first time in the present work as $11\pm4\%$. Combining this value with the absolute feeding intensities of the levels deduced in the above interpretation, $21.7\pm10.4\%$ of the β-decay strength remains unaccounted for, the majority of which presumably feeds the ground state of ^{26}Ne directly, as suggested by shell model calculations. The feeding intensities and logft values deduced for each level are presented in Table VI, from which it can be seen that all of the decay strengths are consistent with allowed β-decay transitions.

TABLE VI. Energies and feeding intensities of levels in ^{26}Ne deduced from the β decay of ^{26}F, corrected for the β-delayed γ-ray detection efficiency. The Q_β value between ground states has been taken as $17\,858\pm135$ keV [23] in the calculation of the logft values.

E_{level} (keV)	Feeding intensity (%)	logft
3691.2 ± 0.3	18.7 ± 2.2	4.69 ± 0.11
2018.2 ± 0.1	48.6 ± 6.6	4.53 ± 0.13
0	21.7 ± 10.4	5.15 ± 0.35

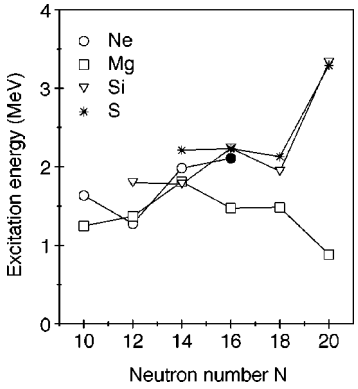

FIG. 9. Excitation energies of the lowest-lying 2^+ states in even-even isotopes of neon (circles), magnesium (squares), silicon (triangles), and sulphur (stars). The energy of the 2^+ state in ^{26}Ne measured for the first time in the present work is indicated by the filled circle. The lines are drawn to guide the eye along isotopic chains.

The structure of $^{26}_{10}\text{Ne}_{16}$ is of particular interest since the nucleon numbers 10 and 16 are both predicted correspond to deformed shell gaps with a major to minor axis ratio of 2:1, or a β_2 deformation parameter of 0.6 [27,28]. In the case of ^{32}Mg, which has a deformed ground state with $\beta_2\approx0.5$, the excitation energy of the lowest-lying 2^+ level is significantly lower than in neighboring even-even magnesium isotopes. The excitation energy measured for the 2^+ level in ^{26}Ne is comparable with the known value for ^{24}Ne (see Fig. 9), suggesting that the ground state of ^{26}Ne does not correspond to the expected deformed configuration. Mass measurements also reveal no binding energy anomaly in the case of ^{26}Ne, in contrast to the deformed nuclide ^{32}Mg [4,7], although a recent shell model calculation predicts a value of $\beta_2\approx0.4$ for the lowest 2^+ state in ^{26}Ne, indicating that this state at least is highly deformed [29].

D. The decays of ^{27}F and ^{29}F

The energy spectrum of β-delayed γ rays for ^{27}F shown in Fig. 10 reveals a single γ-ray line at an energy of 2018 keV, the energy of the $2^+\rightarrow0^+$ transition in ^{26}Ne identified above. This is compatible with the β-delayed neutron emission probability for ^{27}F of $90^{+10}_{-30}\%$ measured for the first time in the present work. The absolute intensity measured for this γ-ray line of $18.0\pm3.2\%$ gives an indication of the relative population of the ground state and excited states in the neutron emission process. These observations are consistent with the low neutron separation energy of 1408 ± 106 keV for ^{27}Ne [23] and shell model calculations, which predict that no excited levels below this threshold are strongly populated in the β decay.

The half-lives measured for ^{27,29}F in the present work were 6.5 ± 1.1 ms and 2.9 ± 0.8 ms, respectively, which compare well with the previously reported values [1,16] (see Table I).

E. The decay of ^{28}Ne

Of the γ rays associated with ^{28}Ne ions in the spectra of Fig. 11, those at 1473 keV and 2389 keV are the most in-

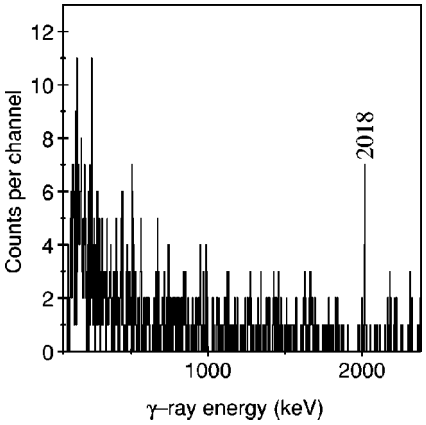

FIG. 10. Energy spectrum of all β-delayed γ rays occurring within 30 ms of the arrival of a ^{27}F ion at the focal plane of LISE3. The γ-ray line at 2018 keV corresponds to the $2^+ \rightarrow 0^+$ transition in ^{26}Ne emitted following β-delayed neutron emission.

tense γ rays known in the decay of ^{28}Na to ^{28}Mg ($t_{1/2} = 34.1 \pm 0.6$ ms) [25]. The decay curves obtained by gating on the remaining lines at 865 keV and 2063 keV are mutually consistent and fitting these combined data yields a half-life of 18 ± 3 ms. This value is consistent with the previously measured values for ^{28}Ne (see Table I), so these γ rays are assigned to the decay of ^{28}Ne and their energies and intensities are summarized in Table VII.

The β-delayed neutron emission probability of ^{28}Ne was determined as $11 \pm 3\%$ (see Table I), which is comparable with the γ-ray line intensities. Although it is in principle

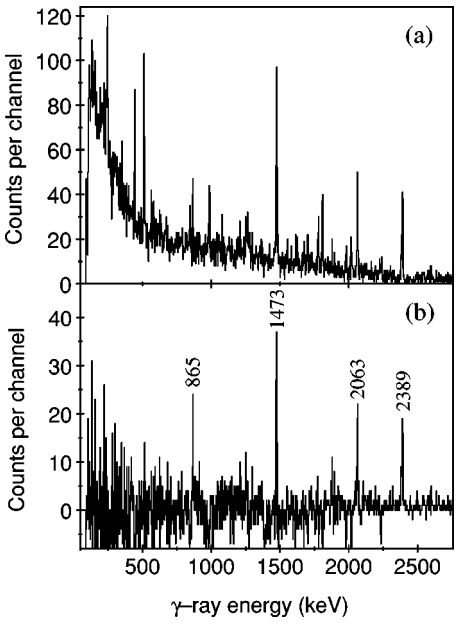

FIG. 11. Energy spectra of (a) all β-delayed γ rays occurring within 50 ms of the arrival of a ^{28}Ne ion at the focal plane of LISE3; (b) the same spectrum after the subtraction of a normalized fraction of the total β-delayed γ-ray spectrum obtained at the same LISE3 settings as these data. γ-ray peaks associated with the β decay of ^{28}Ne and its daughter ^{28}Na are labeled according to their energy in keV.

TABLE VII. Energies and intensities of γ rays observed in the β decay of ^{28}Ne, corrected for the β-delayed γ-ray detection efficiency.

E_γ (keV)	I_γ (relative)	I_γ (per 100 decays)
864.5 ± 0.4	17.5 ± 2.3	3.3 ± 0.4
2062.9 ± 0.3	100.0 ± 6.0	19.0 ± 1.2

possible that the γ rays are emitted from levels in ^{27}Na rather than ^{28}Na, the widths of the 865 keV and 2063 keV γ-ray lines show no sign of Doppler broadening. Furthermore, the absence in Fig. 11 of any γ ray that could correspond to the decay of the first excited state in ^{27}Na at 1.72 ± 0.04 MeV identified using the ^{26}Mg(^{18}O,^{17}F)^{27}Na reaction [8] leads us to assign tentatively these γ rays as emanating from ^{28}Na.

Since ^{27}Na is the heaviest sodium isotope studied using transfer reactions, the γ rays assigned to heavier isotopes can only be compared with shell model calculations. The level scheme calculated using the USD interaction is shown in Fig. 12. The ground state spin and parity of ^{28}Na has been determined to be 1^+ [25,26], rather than 2^+.

Below the one neutron separation energy of 3524 ± 85 keV [23], the shell model calculations predict the existence of three more excited 1^+ levels, of which the two higher-lying states are predicted to have lower logft values. No strong evidence could be found for a γ-ray line at around 1.6 MeV that could represent the decay of the predicted level at 1658 keV to the ground state, or for transitions to the pre-

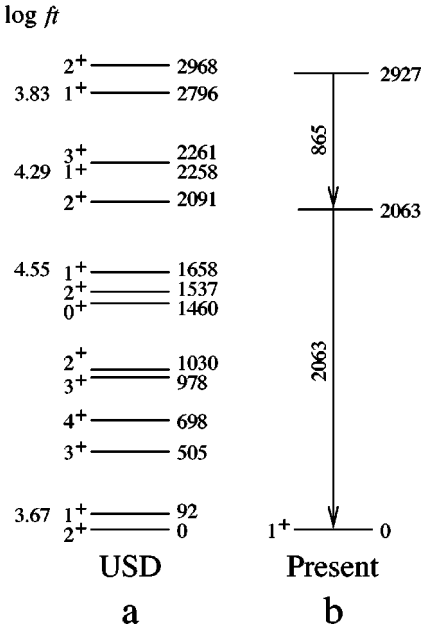

FIG. 12. Comparison of (a) energy levels of ^{28}Na predicted using the shell model with the USD interaction [21], including calculated logft values, with (b) the tentative partial level scheme deduced in the present work. The excitation energies of the levels and γ-ray transition energies are given to the nearest keV.

TABLE VIII. Energies and feeding intensities of levels tentatively deduced from the γ rays observed in the β decay of ^{28}Ne to ^{28}Na, corrected for the β-delayed γ-ray detection efficiency and the average β-delayed neutron emission probability of $16.4\pm2.1\%$ taken from previous measurements and the present work. The Q_β value between ground states has been taken as $12\,312\pm136$ keV [23] in the calculation of the logft values.

E_{level} (keV)	Feeding intensity (%)	logft
2927.4 ± 0.5	3.3 ± 0.4	4.81 ± 0.19
2062.9 ± 0.3	15.7 ± 1.2	4.32 ± 0.11
0	64.5 ± 2.5	4.11 ± 0.10

dicted low-lying 2^+ level. We therefore propose the tentative partial level scheme shown in Fig. 12, which agrees well with the shell model calculations.

Adopting this tentative level scheme, the feeding intensities and logft values deduced are presented in Table VIII. The direct β-decay feeding of the ground state has been assumed to account for all of the unobserved decay strength in this table and results in a reasonable logft value, although the unobserved feeding of the predicted 1658 keV level and any fragmentation of the γ decays of the higher-lying 1^+ states will serve to reduce the feeding of the ground state and hence increase the logft value.

F. The decay of ^{29}Ne

The energy spectra of β-delayed γ rays for ^{29}Ne are shown in Fig. 13. None of the γ-ray lines corresponds with

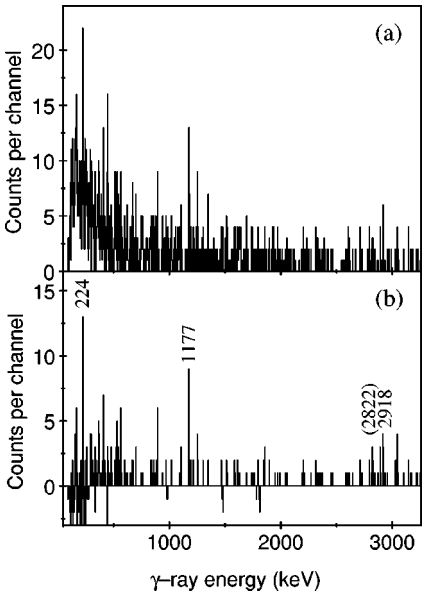

FIG. 13. Energy spectra of (a) all β-delayed γ rays occurring within 50 ms of the arrival of a ^{29}Ne ion at the focal plane of LISE3; (b) the same spectrum after the subtraction of a normalized fraction of the total β-delayed γ-ray spectrum obtained at the same LISE3 settings as these data. The γ rays associated with the β decay of ^{29}Ne are labeled with their energy in keV.

TABLE IX. Energies and intensities of γ rays observed in the β decay of ^{29}Ne, corrected for the β-delayed γ-ray detection efficiency.

E_γ (keV)	I_γ (relative)	I_γ (per 100 decays)
223.8 ± 0.7	18.7 ± 5.5	10.2 ± 1.8
1176.5 ± 1.0	32.8 ± 9.4	17.9 ± 2.9
2918.2 ± 1.5	100.0 ± 23.5	54.7 ± 12.9

the known γ rays from the decay of the daughter nuclide ^{29}Na [25] or to those tentatively assigned to transitions in ^{28}Na in the previous section. These γ rays are therefore tentatively assigned to transitions in ^{29}Na and their energies and absolute intensities are presented in Table IX.

The 2918 keV γ ray accounts for 55% of the total decay strength and is significantly more intense than the other two γ-ray lines. The ground state spin of ^{29}Na has been determined as 3/2 from laser measurements [26] and has been assigned as having even parity [25], whereas shell model calculations using the USD interaction place the lowest $3/2^+$ level 137 keV above a predicted $5/2^+$ ground state. Consequently there is a possibility that this low-lying $5/2^+$ state could be fed by the γ-ray transitions and its γ decays to the true ground state are too low in energy to be observed. A weak candidate γ-ray line at an energy of 2822.4 ± 2.7 keV was identified with an intensity of $13.0\pm9.5\,\gamma$ rays per 100 β decays. If this γ ray were to represent the decay of a 2918 keV level to the $5/2^+$ state and the 2918 keV γ ray fed the ground state directly, one would expect to see a 96 keV γ-ray line, but no evidence for this could be found. (The 96 keV γ-ray transition in ^{19}O observed in the β decay of ^{20}N with an intensity of 30 ± 5 γ rays per 100 β decays was clearly evident in the present experiment at a different LISE3 setting.) This potential ambiguity cannot be resolved with the low level of statistics in this case and therefore prevents the construction of a level scheme for ^{29}Na.

The half-life of ^{29}Ne was determined as 19 ± 9 ms, which is consistent with the recently remeasured values (see Table I). The β-delayed neutron emission probability of ^{29}Ne was determined for the first time in the present work as $27\pm9\%$.

G. The decay of ^{30}Ne

Direct mass measurements [4] indicate that the inversion in shell model level sequences observed for the $N=20$ isotones ^{31}Na and ^{32}Mg may persist for ^{30}Ne. This conclusion is supported by several large scale shell model calculations [30–33] and has important implications for the decay properties of ^{30}Ne. The ground state of ^{30}Ne is expected to have a majority intruder $(2\hbar\omega)$ character, whereas the ground state of ^{30}Na is mostly an sd shell $(0\hbar\omega)$ configuration [33,34]. Consequently one would expect that the β decays of the ground state of ^{30}Ne should mainly populate the $2\hbar\omega$ states in ^{30}Na.

A single γ-ray line at an energy of 150.6 ± 0.2 keV is clearly evident in the β-delayed γ-ray energy spectrum for

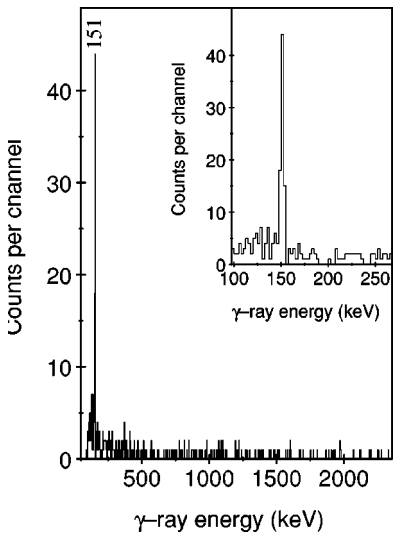

FIG. 14. Energy spectrum of all β-delayed γ rays occurring within 30 ms of the arrival of a ^{30}Ne ion at the focal plane of LISE3. The γ-ray line assigned to the decay of ^{30}Ne is labeled with its energy in keV. The inset shows a portion of the energy spectrum in the region around this γ-ray line.

^{30}Ne. This transition accounts for $95\pm10\%$ of the decay intensity but is not known from the decay of ^{30}Na [25]. The β-delayed neutron emission probability of ^{30}Ne was measured for the first time in the present work as $9^{+17}_{-9}\%$, indicating that this γ-ray line must represent a transition in ^{30}Na. The half-life measured for this γ-ray line was 7 ± 2 ms, which agrees with the previous measurements for ^{30}Ne (see Table I).

The lowest energy $0\hbar\omega$ and $2\hbar\omega$ levels in ^{30}Na calculated using the WBMB interaction [32] are shown in Fig. 14. The 1^+ level predicted to lie 201 keV above the 2^+ lowest $2\hbar\omega$ state is expected from the calculations to have the strongest direct feeding by an allowed β decay from the ground state of ^{30}Ne, so we tentatively attribute the γ ray identified in the present work to the decay of this 1^+ level to the 2^+ state.

The excitation energy of the lowest-lying $2\hbar\omega$ state above the $0\hbar\omega$ ground state in ^{30}Na is calculated to be 1423 keV in the present work, which compares with the previous estimates of 1.9 MeV in Ref. [31], 0.8 MeV in Ref. [32], and 1.04 MeV in Ref. [33]. The spin of the ground state has been determined to be $2\hbar$ [26] and in principle one would expect the lowest $2\hbar\omega$ state eventually to decay by some path to this $0\hbar\omega$ ground state. However, no evidence could be found in the spectrum of Fig. 15 for any connecting transition, although this may simply reflect the comparatively low number of nuclei collected, the lower detection efficiency for higher energy γ rays and a possibly fragmented decay path between the states.

Taking the average of the estimates of the excitation energy of the $2\hbar\omega$ state in ^{30}Na and assuming that all of the observed strength arises as a result of direct β-decay feeding of the level, the logft value would be ~3.5, which is consistent with an allowed transition. Given that the one neutron separation energy of ^{30}Na is 2096 ± 128 keV [23] and the next excited $2\hbar\omega$ 1^+ state is calculated to lie around 2 MeV above the $2\hbar\omega$ ''ground state,'' the conclusion that the observed transition represents essentially all of the strength not involving neutron emission is entirely consistent with the shell model calculations.

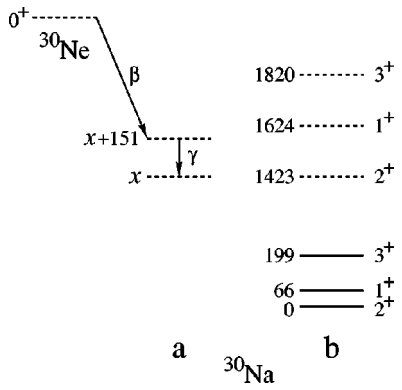

FIG. 15. Comparison of (a) the tentative experimental level scheme for ^{30}Na with (b) shell model estimates of the lowest energy $0\hbar\omega$ and $2\hbar\omega$ levels calculated using the WBMB interaction [32]. The solid lines represent the energies of $0\hbar\omega$ levels, while $2\hbar\omega$ levels are indicated by the dashed lines. The relative energies of the lowest-lying $0\hbar\omega$ and $2\hbar\omega$ levels, denoted here by x, is unknown in ^{30}Na. See text for details of theoretical estimates of this quantity.

IV. CONCLUSION

We have presented the first β-delayed γ-ray measurements for 7 nuclides (^{24}O, $^{25-27}$F, $^{28-30}$Ne) residing close to the neutron drip line and measured their half-lives and neutron emission probabilities. The γ-ray spectra have been interpreted through comparisons with shell model calculations and level schemes obtained from transfer reaction measurements, where available. Some of the nuclides investigated here are also the subject of Coulomb excitation and in-beam fragmentation γ-ray measurements [35] which potentially provide complementary information, as well as the prospect of measuring excited levels in nuclei such as ^{30}Ne where the β-decay precursors are unbound. Increases in the primary beam intensity and γ-ray detection efficiency soon to be available will offer new opportunities for extending the present studies. In the more distant future it is conceivable that accelerated radioactive beams could herald the renaissance of transfer reactions being used to probe the energy level structure of extremely neutron rich nuclei [36].

ACKNOWLEDGMENTS

We are grateful for the excellent beams and technical support provided by the staff at GANIL. This work was supported by EPSRC (UK), IN2P3 and CEA (France); the European Community under Contract No. ERBFMGECT 950036 (Human Capital and Mobility, Access to the GANIL Large Scale Facility); the Czech Academy of Science (Grant A 1048 605). R.G.A., S.M.V., and R.D.P. acknowledge EPSRC support. P.H.R. acknowledges support from the Nuffield Foundation and the British Council.

[1] O. Tarasov, R. Allatt, J. C. Angélique, R. Anne, C. Borcea, Z. Dlouhý, C. Donzaud, S. Grévy, D. Guillemaud-Mueller, M. Lewitowicz, S. Lukyanov, A.C. Mueller, F. Nowacki, Yu. Oganessian, N.A. Orr, A.N. Ostrowski, R.D. Page, Yu. Penionzhkevich, F. Pougheon, A. Reed, M.G. Saint-Laurent, W. Schwab, E. Sokol, O. Sorlin, W. Trinder, and J. S. Winfield, Phys. Lett. B **409**, 64 (1997).

[2] H. Sakurai, S.M. Lukyanov, M. Notani, N. Aoi, D. Beaumel, N. Fukuda, M. Hirai, E. Ideguchi, N. Imai, M. Ishihara, H. Iwisaki, T. Kubo, K. Kusaka, H. Kumagai, T. Nakamura, H. Ogawa, Yu.E. Penionzhkevich, T. Teranishi, Y.X. Watanabe, K. Yoneda, and A. Yoshida, *Proceedings of the Second International Conference on Exotic Nuclei and Atomic Masses*, Shanty Creek Resort, Bellaire, Michigan, 1998, AIP Conf. Proc. 455 (AIP, New York, 1999), p. 37.

[3] J.M. Wouters, R.H. Kraus, Jr., D.J. Vieira, G.W. Butler, and K.E.G. Löbner, Z. Phys. A **331**, 229 (1988).

[4] N.A. Orr, W. Mittig, L.K. Fifield, M. Lewitowicz, E. Plagnol, Y. Schutz, Zhan Wen Long, L. Bianchi, A. Gillibert, A.V. Belozyorov, S.M. Lukyanov, Yu.E. Penionzhkevich, A.C.C. Villari, A. Consulo, A. Foti, G. Audi, C. Stephan, and L. Tassan-Got, Phys. Lett. B **258**, 29 (1991).

[5] P.M. Endt, Nucl. Phys. **A521**, 1 (1990).

[6] K.H. Wilcox, N.A. Jelley, G.J. Wozniak, R.B. Weisenmiller, H.L. Harney, and J. Cerny, Phys. Rev. Lett. **30**, 866 (1973).

[7] H. Nann, K.K. Seth, S.G. Iversen, M.O. Kaletka, D.B. Barlow, and D. Smith, Phys. Lett. **96B**, 261 (1980).

[8] L.K. Fifield, P.V. Drumm, M.A.C. Hotchkis, T.R. Ophel, and C.L. Woods, Nucl. Phys. **A437**, 141 (1985).

[9] C.L. Woods, L.K. Fifield, R.A. Bark, P.V. Drumm, and M.A.C. Hotchkis, Nucl. Phys. **A437**, 454 (1985).

[10] N.A. Orr, L.K. Fifield, W.N. Catford, and C.L. Woods, Nucl. Phys. **A491**, 457 (1989).

[11] R. Anne, D. Bazin, A.C. Mueller, J.C. Jacmart, and M. Langevin, Nucl. Instrum. Methods Phys. Res. A **257**, 215 (1987).

[12] E.A. Sokol, V.I. Smirnov, S.M. Lukyanov, and Yu.E. Penionzhkevich, Nucl. Instrum. Methods Phys. Res. A **400**, 96 (1997).

[13] C.W. Beausang, S.A. Forbes, P. Fallon, P.J. Nolan, P.J. Twin, J.N. Mo, J.C. Lisle, M.A. Bentley, J. Simpson, F.A. Beck, D. Curien, G. de France, G. Duchêne, and D. Popescu, Nucl. Instrum. Methods Phys. Res. A **313**, 37 (1992).

[14] A.C. Mueller, D. Guillemaud-Mueller, J.C. Jacmart, E. Kashy, F. Pougheon, A. Richard, A. Staudt, H.V. Klapdor-Kleingrothaus, M. Lewitowicz, R. Anne, P. Bricault, C. Détraz, Yu.E. Penionzhkevich, A.G. Artukh, A.V. Belozyorov, S.M. Lukyanov, D. Bazin, and W.D. Schmidt-Ott, Nucl. Phys. **A513**, 1 (1990).

[15] P.L. Reeder, R.A. Warner, W.K. Hensley, D.J. Vieira, and J.M. Wouters, Phys. Rev. C **44**, 1435 (1991).

[16] M. Notani, N. Aoi, N. Fukuda, M. Ishihara, H. Iwasaki, H. Ogawa, T. Kubo, S.M. Lukyanov, T. Nakamura, Yu.E. Penionzhkevich, H. Sakurai, T. Teranishi, Y.X. Watanabe, K. Yoneda, and A. Yoshida, RIKEN Accelerator Progress Report **31**, 71 (1998).

[17] O. Tengblad, M.J.G. Borge, L. Johannsen, B. Jonson, M. Lindroos, T. Nilsson, G. Nyman, A. Poves, H.L. Ravn, J. Retamosa, K. Riisager, P. Sona, K. Wilhelmsen, and ISOLDE Collaboration, Z. Phys. A **342**, 303 (1992).

[18] J.P. Dufour, R. Del Moral, A. Fleury, F. Hubert, D. Jean, M.S. Pravikoff, H. Delagrange, H. Geissel, and K.-H. Schmidt, Z. Phys. A **324**, 487 (1986).

[19] B.A. Brown, A. Etchegoyen, and W.D.M. Rae, OXBASH, The Oxford-Buenos Aires-MSU shell model code, Michigan State University Cyclotron Laboratory Report No. 524, 1988.

[20] W. Chung, Ph.D. thesis, Michigan State University, 1976.

[21] B.H. Wildenthal, Prog. Part. Nucl. Phys. **11**, 5 (1984).

[22] B.A. Brown, W.A. Richter, R.E. Julies, and B.H. Wildenthal, Ann. Phys. (N.Y.) **182**, 191 (1988).

[23] G. Audi and A.H. Wapstra, Nucl. Phys. **A595**, 409 (1995).

[24] D.R. Goosman, D.E. Alburger, and J.C. Hardy, Phys. Rev. C **7**, 1133 (1973).

[25] D. Guillemaud-Mueller, C. Détraz, M. Langevin, F. Naulin, M. de Saint-Simon, C. Thibault, F. Touchard, and M. Epherre, Nucl. Phys. **A426**, 37 (1984).

[26] G. Huber, F. Touchard, S. Büttgenbach, C. Thibault, R. Klapisch, H.T. Duong, S. Liberman, J. Pinard, J.L. Vialle, P. Juncar, and P. Jacquinot, Phys. Rev. C **18**, 2342 (1978).

[27] R.K. Sheline, I. Ragnarsson, and S.G. Nilsson, Phys. Lett. **41B**, 115 (1972).

[28] I. Ragnarsson, S. Åberg, and R.K. Sheline, Phys. Scr. **24**, 215 (1981).

[29] T. Siiskonen, P.O. Lipas, and J. Rikovska, Phys. Rev. C (submitted).

[30] N. Fukunishi, T. Otsuka, and T. Sebe, Phys. Lett. B **296**, 279 (1992).

[31] A. Poves and J. Retamosa, Nucl. Phys. **A571**, 221 (1994).

[32] E.K. Warburton, J.A. Becker, and B.A. Brown, Phys. Rev. C **41**, 1147 (1990).

[33] E. Caurier, F. Nowacki, A. Poves, and J. Retamosa, Phys. Rev. C **58**, 2033 (1998).

[34] A. Poves and J. Retamosa, Phys. Lett. B **184**, 311 (1987).

[35] F. Azaiez, M. Belleguic, O. Sorlin, S. Leenhardt, M.G. Saint-Laurent, M.J. Lopez, J.C. Angélique, C. Borcea, C. Bourgeois, J.M. Daugat, I. Deloncle, C. Donzaud, J. Duprat, G. de France, A. Gillibert, S. Grévy, D. Guillemaud-Mueller, J. Kiener, M. Lewitowicz, F. Marie, W. Mittig, A.C. Mueller, F. De Oliveira, N. Orr, Yu.E. Penionzhkevich, F. Pougheon, M.G. Porquet, P. Roussel-Chomaz, H. Savajols, W. Shuying, Yu. Sobolev, and J. Winfield, Proceedings of Nuclear Structure '98, Gatlinburg, Tennessee, 1998 (in press).

[36] J.S. Winfield, W.N. Catford, and N.A. Orr, Nucl. Instrum. Methods Phys. Res. A **396**, 147 (1997).